A&A 484, 413–418 (2008)
DOI: 10.1051/0004-6361:20078381

Astronomy & Astrophysics

Confirmation of the binary status of Chamaeleon Hα 2 – a very young low-mass binary in Chamaeleon*,**

T. O. B. Schmidt[1], R. Neuhäuser[1], N. Vogt[2,3], A. Seifahrt[1], T. Roell[1], and A. Bedalov[1]

[1] Astrophysikalisches Institut und Universitäts-Sternwarte, Universität Jena, Schillergäßchen 2-3, 07745 Jena, Germany
e-mail: tobi@astro.uni-jena.de
[2] Departamento de Física y Astronomía, Universidad de Valparaíso, Avenida Gran Bretaña 1111, Valparaíso, Chile
[3] Instituto de Astronomía, Universidad Catolica del Norte, Avda. Angamos 0610, Antofagasta, Chile

Received 30 July 2007 / Accepted 29 January 2008

ABSTRACT

Context. Neuhäuser & Comerón (1998, Science, 282, 83; 1999, A&A, 350, 612) presented direct imaging evidence, as well as first spectra, of several young stellar and sub-stellar M6- to M8-type objects in the Cha I dark cloud. One of these objects is Cha Hα 2, classified as brown dwarf candidate in several publications and suggested as possible binary in Neuhäuser et al. (2002, A&A, 384, 999).
Aims. We have searched around Cha Hα 2 for close and faint companions with adaptive optics imaging.
Methods. Two epochs of direct imaging data were taken with the Very Large Telescope (VLT) Adaptive Optics instrument NACO in February 2006 and March 2007 in *Ks*-band together with a Hipparcos binary for astrometric calibration. Moreover, we took a *J*-band image in March 2007 to get color information. We retrieved an earlier image from 2005 from the European Southern Observatory (ESO) Science Archive Facility, increasing the available time coverage. After confirmation of common proper motion, we deduce physical parameters of the objects by spectroscopy, like temperature and mass.
Results. We find Cha Hα 2 to be a very close binary of ∼0.16 arcsec separation, having a flux ratio of ∼0.91, thus having almost equal brightness and indistinguishable spectral types within the errors. We show that the two tentative components of Cha Hα 2 form a common proper motion pair, and that neither component is a non-moving background object. We even find evidence for orbital motion. A combined spectrum of both stars spanning optical and near-infrared parts of the spectral energy distribution yields a temperature of 3000 ± 100 K, corresponding to a spectral type of M6 ± 1 and a surface gravity of $\log g = 4.0^{+0.75}_{-0.5}$, both from a comparison with GAIA model atmospheres. Furthermore, we obtained an optical extinction of $A_V \simeq 4.3$ mag from this comparison.
Conclusions. We derive masses of ∼0.110 $M_\odot$ (≥0.070 $M_\odot$) and ∼0.124 $M_\odot$ (≥0.077 $M_\odot$) for the two components of Cha Hα 2, i.e., probably low-mass stars, but one component could possibly be a brown dwarf.

Key words. stars: low-mass, brown dwarfs – stars: binaries: close – stars: binaries: visual – stars: individual: Cha Hα 2

1. Introduction

Neuhäuser & Comerón (1998) found Cha Hα 2, also called ISO-ChaI 111, to be a member of the Cha I star-forming cloud with an age of ∼2 Myr. Neuhäuser & Comerón (1999) then classified Cha Hα 2 as a candidate brown dwarf of spectral type M6.5, using medium-resolution optical spectroscopy. Comerón et al. (2000) presented evidence for near- to mid-infrared excess indicating a disk. Natta & Testi (2001) and Apai et al. (2002) argued that the spectrum can be explained with an optically flat dust disk, but not with a flared disk, due to lack of any prominent silicate feature previously expected for the disk of Cha Hα 2. Neuhäuser et al. (2002) searched for companions around Cha Hα 1−12 with the Hubble Space Telescope and presented the first indication for binarity of Cha Hα 2 due to elongation of the Point Spread Function (PSF) in filters *R* and Hα.

The rotational period of 3.21 ± 0.17 days, found in photometric data by Joergens et al. (2003), confirmed the spectroscopic period of $2.9^{+1.4}_{-1.0}$ days already proposed in Joergens & Guenther (2001). Natta et al. (2004) observed nine stars in the Cha I dark cloud and found only at Cha Hα 2 signs of accretion in H α and Paβ, making it the only object out of nine to show clear signs of accretion at a rate of $\sim 10^{-10}$ $M_\odot$/yr and an inclination of ∼65 to 75°. Observations with XMM-Newton by Stelzer et al. (2004) revealed X-ray emission from Cha Hα 2. Recently, Apai et al. (2005) succeeded in using new infrared spectra to conclude that the disk around Cha Hα 2 is still closer to the flat disk model, even though a prominent enstatite silicate feature could be found at 9.3 μm.

Here, we present evidence for the binarity of Cha Hα 2. In Sects. 2 and 3, we present the observations, data reduction, and astrometric results. The available photometric properties of both components will be discussed in Sect. 4. The spectroscopy of the system is presented in Sect. 5. We end with conclusions in Sect. 6.

2. Observations with VLT/NACO

We observed Cha Hα 2 in two epochs in February 2006 and in March 2007, see Table 1 for the observations log. Included in Table 1 are the data found in the archive from March 2005.

⋆ Based on observations made with ESO telescopes at the Paranal Observatory under programme IDs 076.C-0292A, 076.C-0339B, 078.C-0535A, at the La Silla Observatory under programme ID 065.L-0144B, the Hubble Space Telescope under programme ID GO-8716 and on observations made with the European Southern Observatory telescopes obtained from the ESO/ST-ECF Science Archive Facility.
⋆⋆ Color version of Fig. 6 is only available in electronic form at http://www.aanda.org

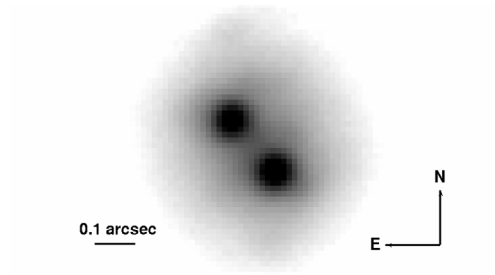

Fig. 1. NACO *Ks*-band image of the low-mass binary Cha Hα 2 from 25 March 2005. The southwestern component appears slightly brighter, hence we call this component A (or SW), the fainter northeastern component B (or NE).

Table 1. VLT/NACO observations log.

JD – 2453400 [days]	Date of observation	DIT [s]	NDIT	No. (a) images	Filter
54.62360 (b)	25 Mar. 2005	30	2	23	*Ks*
382.67884	16 Feb. 2006	10	6	20	*Ks*
760.70760	1 Mar. 2007	60	2	15	*Ks*
761.66193	2 Mar. 2007	30	2	24	*J*

Remarks: (a) Each image consists of the number of exposures given in Col. 4 times the individual integration time given in Col. 3. (b) Retrieved from the ESO Science Archive Facility.

Table 2. Proper motions of Cha Hα 2.

Source	PM RA [mas/yr]	PM Dec [mas/yr]
USNO-B1 (a)	–20 ± 17	–14 ± 4
PSSPMC (b)	–23 ± 17	+1 ± 17
SSS-FORS1	–19.4 ± 14.9	–0.3 ± 14.9
SSS-SofI	–23.0 ± 14.1	+7.8 ± 14.1
Mean	–21.8 ± 8.8	+3.2 ± 8.8

Remarks: (a) This value (Monet et al. 2003) was not used in the final proper motion due to its unreasonably small error of PM in declination, which makes it inconsistent with the measurements using the SuperCOSMOS Sky Survey in comparison to data from the New Technology Telescope (NTT) instrument Son of ISAAC (SSS-SofI). (b) From the Pre-main Sequence Stars Proper Motion Catalog (Ducourant et al. 2005).

We observed with the European Southern Observatory (ESO) Very Large Telescope (VLT) instrument Naos-Conica (NACO, Lenzen et al. 2003; Rousset et al. 2003). DIT, NDIT, NINT, and filter bands are listed in Table 1. In all cases, we used the S13 camera (~13 mas/pixel pixel scale) and the double-correlated read-out mode.

For the raw data reduction, we subtracted a mean dark from all the science frames and flatfield frames, then divided by the mean dark-subtracted flatfield and subtracted the mean background using *eclipse/jitter*.

In all three images, Cha Hα 2 is clearly resolved in a double object with an apparent separation of ~160 mas at a position angle of ~40°, see Fig. 1. The southwestern component appears slightly brighter, hence we call this component A (or SW), the fainter northeastern component B (or NE).

3. Astrometry

To check for common proper motion of the two tentative components of Cha Hα 2, we used the proper motion (here PM) of

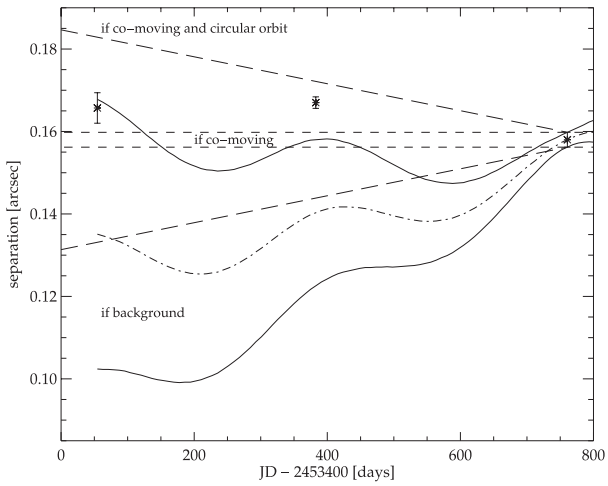

Fig. 2. Observed separation between the two components of Cha Hα 2. The archival data point from 2005 and our two measurements from 2006 and 2007 are shown. The short-dashed lines enclose the area for constant separation. The dash-dotted line is the change expected if the B component is a non-moving background star. The opening cone enclosed by the solid lines are its estimated errors. The waves of this cone show the differential parallactic motion, which has to be taken into account if the other component is a non-moving background star. The opening long-dashed cone indicates the amplitude of possible orbital motion.

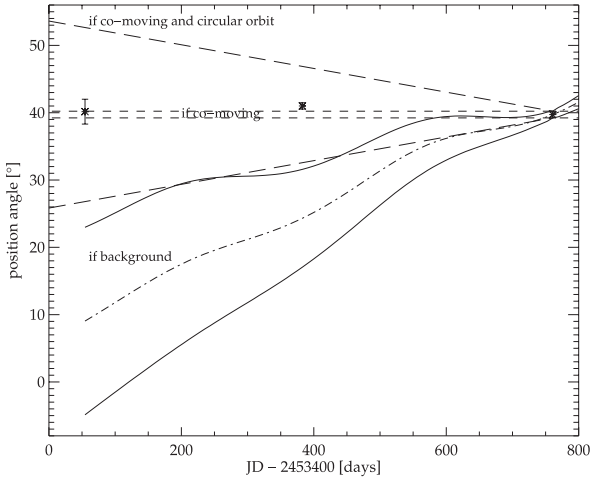

Fig. 3. Observed position angle between the two components of Cha Hα 2 (measured from the brighter component north over east to south). See Fig. 2 for details.

Cha Hα 2 published in the literature (USNO-B and PSSPMC); we calculated additional values by comparing SuperCOSMOS Sky Survey (here SSS) data from 1985 with images from VLT/FORS1 (epoch 1999, published by Comeron et al. 2000, obtained directly from F. Comerón, priv. com.) and New Technology Telescope instrument Son of ISAAC (NTT/SofI) from 2000, observed by us (10 × 50 × 1.2 s integrations), reduced in the same way as the NACO data with eclipse. See Table 2 for the results (originally from Gaedke 2005, but revised here by us). We use the mean proper motion for checking, whether the two objects show common proper motion below.

We calibrated the NACO data using the wide binary star HIP 73357 for our two measurements in 2006 and 2007, and the closer binary HIP 73111 for which we found archived data taken in the same night as the Cha Hα 2 observations in 2005,

Table 3. Astrometric calibration and astrometric results for Cha Hα 2 AB.

JD – 2453400 [days]	Calibration binary	Pixel scale [mas/pixel]	Orientation [deg]	JD – 2 453 400 [days]	Target	Separation [mas]	PA (a) [deg]
54.76919	HIP 73111	13.22 ± 0.28	–0.17 ± 1.84	54.62360	Cha Hα 2 AB	165.7 ± 3.7	40.16 ± 1.84
388.84537	HIP 73357	13.24 ± 0.07	0.18 ± 0.46	382.67884	Cha Hα 2 AB	167.0 ± 1.4	41.01 ± 0.47
760.76369	HIP 73357	13.24 ± 0.07	0.34 ± 0.46	760.70760	Cha Hα 2 AB	158.0 ± 1.8	39.73 ± 0.50

Remarks: All *K*s-band images. (a) PA is measured from N over E to S. 180 deg to be added to position angle (PA) if seen from fainter component.

resulting in the astrometric calibration summarized in Table 3. The error bars of pixel scale and orientation include, possible orbital motion of the respective binary since its measurement by Hipparcos – i.e., a maximum change in separation due to possible orbital motion for circular edge-on orbit and a maximum change in position angle for circular pole-on orbit – as well as the uncertainties in parallax, total mass, position measurements in our images and separation at the epoch of Hipparcos of the respective binary system.

To determine the positions of both components we constructed a reference PSF from the binary itself by using the undeformed remote sides of both objects shifted to the same peak position. Thus, we obtained a clean reference PSF for each single image. With IDL/starfinder, we scaled and shifted the reference PSF simultaneously to both components in each of our individual images by minimizing the residuals. As a result, we obtained positions (see Table 3) and relative photometry (see Table 4), including realistic error estimates for each object by averaging the results of all single images taken within each epoch.

The development of separation and position angle with time is shown in Figs. 2–5. We can exclude by 0.9σ and 1.5σ (Fig. 2); 2.2σ and 2.3σ (Fig. 3); 1.4σ and 1.0σ (Fig. 4); 2.1σ and 1.9σ (Fig. 5) that either one of the tentative components of Cha Hα 2 is a non-moving background object. Viz, for both components the background hypothesis is rejected by ≥3.7σ, respectively. For two objects slightly above the sub-stellar mass limit (see below) and the given separation (at ∼168 pc), the orbital period is ∼110 yrs, so that the maximum change in separation due to orbital motion (for circular edge-on orbit) is ∼12 mas/yr (∼3°/yr in PA for pole-on orbit). While orbital motion could be detected in PA only from one point in 2006 in contrast to 2007, with 1.9σ significance, we detect orbital motion as deviation of the separation in 2005 and 2006 in contrast to the 2007 measurement, with 1.9σ and 3.9σ significance. From the negligible change in PA during our ∼2 years of epoch difference, we can exclude a circular pole on orbit by 2.8σ, however, we cannot rule out a highly eccentric pole-on orbit.

In Fig. 7, the data from Hubble Space Telescope by Neuhäuser et al. (2002) are also included. Only the plot for the assumption of component B being a non-moving background star is shown here. The Hubble Space Telescope data hence yield another 2.2σ and 2.3σ for component A and B not being a non-moving background star, respectively.

While the difference seen in PA and the separation between the different observations are consistent with common proper motion and some orbital motion, a possible difference in proper motion between both objects of up to a few mas/yr cannot be excluded from the data. Such a difference in proper motion is typical for the velocity dispersion in star forming regions like Cha I (Ducourant et al. 2005), so that we cannot yet exclude that both objects are independent members of Cha I, but not orbiting each other. However, it is extremely unlikely that two objects with almost the same temperatures, *J* and *K* magnitudes, gravities, radii, proper motions, and extinctions are located within less than 170 mas. Even if this would be the case, age, and distance would be the same as assumed below, hence also the mass estimation.

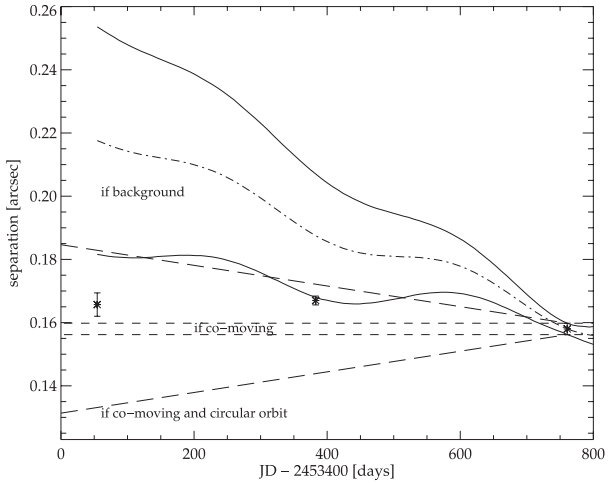

Fig. 4. Observed separation between the two components of Cha Hα 2. Same as Fig. 2, but the opening cone enclosed by the solid lines is the change expected if the A component is a non-moving background star.

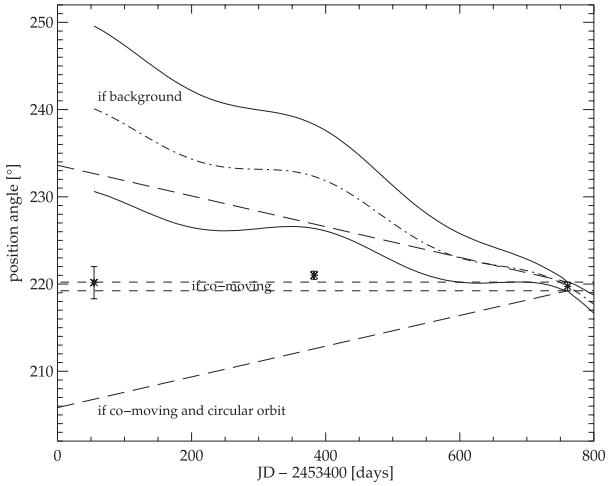

Fig. 5. Same as Fig. 3, but position angle between the two components measured from the B component and assuming the A component is a non-moving background star.

4. Photometry

As described in the last section, we obtained from the PSF fitting of both components also the relative flux ratio, see Table 4. We considered these flux ratios in the astrometric proper motion analysis since the background hypotheses is based on proper

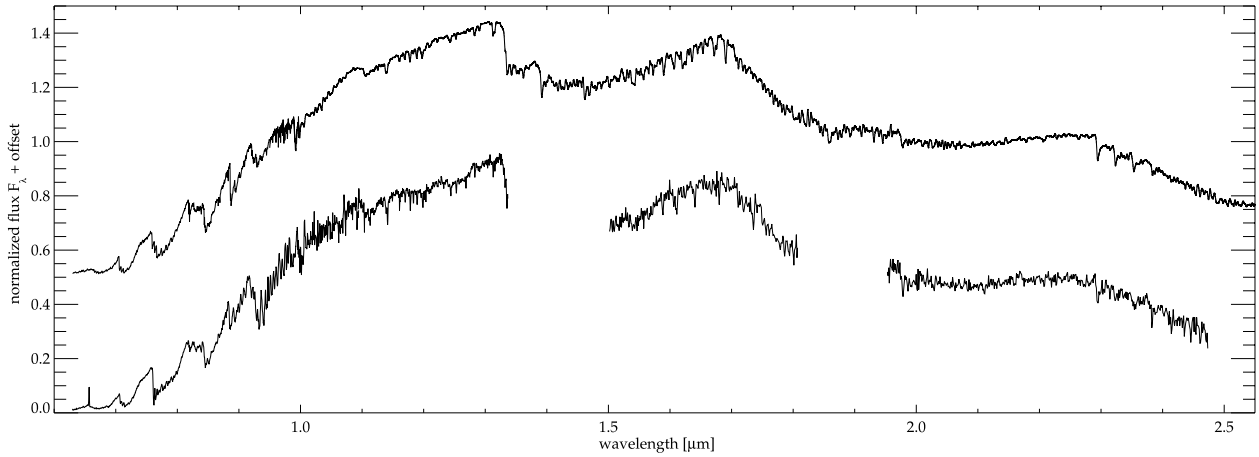

Fig. 6. *Bottom*: spectrum of both components from the optical part to the near-infrared combined from data from Comerón et al. (2000) and data from the ESO Paranal and La Silla instruments ISAAC and SofI retrieved from the ESO Science Archive Facility. *Top*: the best fit to the spectrum: GAIA models computed with the PHOENIX code by Brott & Hauschildt (2005) for a temperature of 3000 K, log g of 4.0 and a visual extinction $A_V \simeq 4.3$ mag. Note that the missing flux depression in J-band (between 1.2 and 1.3 micron) as well as in the peak of the H-band (around 1.65 micron) is due to missing FeH opacities in the spectral models. Note the strong Hα emission in Cha Hα 2 at 0.6568 μm.

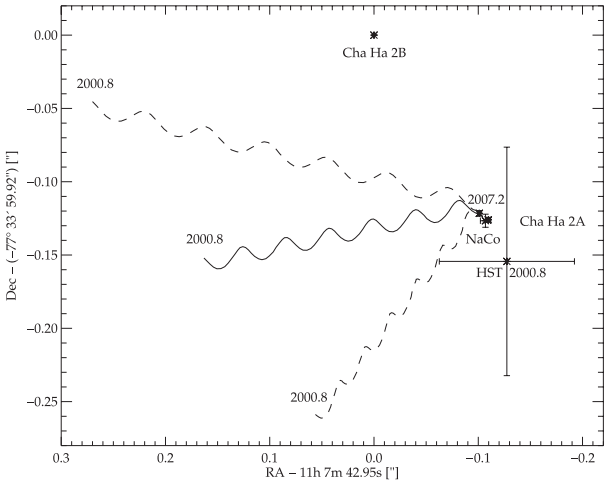

Fig. 7. Plot of the true and expected position of Cha Hα 2 A if Cha Hα 2 B is a non-moving background star. Shown are the NACO measurements from 2005 to 2007, as in Figs. 2–5, and, in addition, the measurement from 2000 using the Hubble Space Telescope in R-band by Neuhäuser et al. (2002). As in Fig. 2, the line showing parallactic wobbles is the expected position of component A if component B is a non-moving background star, in this case from epoch 2000.8 until 2007.2, *from left to right*. The opening dashed cone are its errors. The HST data point obtained at epoch 2000.8 is significantly different (2.3σ) from the expectation, if background.

motions obtained by centroid measurements of the unresolved system. Hence, if one component were a non-moving background object, the centroid (and thus the proper motion of the combined object) would only shift by about half the relative change in separation between both objects.

Using the unresolved photometry of Cha Hα 2 from the Two Micron All Sky Survey (2MASS) catalogue of $J = 12.210 \pm 0.024$ mag and $K = 10.675 \pm 0.021$ mag, we obtain the photometry of each component using our measured flux ratios, see Table 5. We see no evidence for photometric variability.

5. Spectroscopy

We combined all available spectra of Cha Hα 2 from the archive and an optical spectrum obtained directly from F. Comerón (priv. com.) published in Comerón et al. (2000) to create a combined spectrum with a nearly complete coverage from 0.64 μm to 2.45 μm. The data were reduced in a standard manner, doing flat field correction, sky subtraction, spectrum extraction, wavelength calibration, and standard correction with G stars. The spectra are not flux-calibrated. We found the relative offsets from the overlaps of the spectra.

We fitted this spectrum with GAIA COND models computed with the PHOENIX code by Brott & Hauschildt (2005). COND represents the case where dust forms, as in the similar DUSTY models, but rains out completely from the photosphere into deeper layers and, hence, the region where $\tau = 1$ is free of dust. Since little or no dust forms at temperatures above ~2400 K both models with different treatment of dust formation give the same result at the given temperatures. Our best fit results give an effective temperature of 3000 ± 100 K, a surface gravity $\log g = 4.0^{+0.75}_{-0.5}$ and a visual extinction of $A_V = 4.3 \pm 0.25$ mag, see Fig. 6 and the online material for a color version. We note that our extinction value is in between the A_V of 7.9 mag measured in a slope in the A_V map from Kainulainen et al. (2006) and the first ever measured value of 3.55 mag by Neuhäuser & Comerón (1998). Given the quality of our fit, we find here further evidence for the physical binarity of Cha Hα 2 being a double of almost identical mid- to late-M-type objects. If one of the components would be a background (or foreground) object, both the spectral type and the extinction of the components would differ and the unresolved spectrum of the binary would not be consistent with one spectral type over the whole spectral range.

The derived temperature can be converted to a spectral type of M6 ± 1 with the empirical temperature scale for young M-type objects from Luhman (1999). Moreover, our combined spectrum in Fig. 6 resembles very much the spectrum of the M5.75 object ϵ Cha 10 in Luhman (2004).

We also obtained low-S/N (~15) K-band spectra of both objects with VLT/NACO, see Fig. 8. They are indistinguishable, giving further evidence that neither of the two objects are background or foreground stars, which would exhibit a significantly different K-band spectrum.

Table 4. Flux ratios of the Cha Hα 2 system.

JD – 2453400 [days]	Filter	B/A flux ratio
54.62360	*Ks*	0.931 ± 0.024
382.67884	*Ks*	0.908 ± 0.014
760.70760	*Ks*	0.894 ± 0.053
Mean	*Ks*	0.910 ± 0.019
761.66193	*J*	0.893 ± 0.040

Table 5. Brightnesses of the Cha Hα 2 system.

Component	*J*-band	*Ks*-band
Cha Hα 2 A (SW)	12.903 ± 0.033	11.378 ± 0.024
Cha Hα 2 B (NE)	13.026 ± 0.035	11.480 ± 0.024

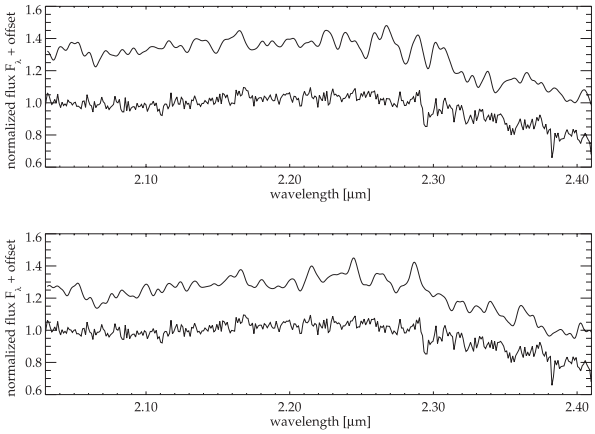

Fig. 8. Observed *K*-band NACO spectra of the Cha Hα 2 system. In each panel, one of the components of the system is shown (*top in each panel*) compared to the higher S/N spectrum of both objects combined from Fig. 6 (*bottom in each panel*). *Top*: component A (southwestern component). *Bottom*: component B (northeastern component). Both spectra are dereddened using the visual extinction of $A_V \simeq 4.3$ mag derived from the spectra shown in Fig. 6.

6. Conclusions

From the photometry, the visual extinction, an extinction law to convert the visual to a near-infrared extinction by Rieke & Lebofsky (1985), a bolometric correction BC_K of 3.0 ± 0.1 mag from Golimowski et al. (2004) and the distance to a particular member of the Cha I cloud of 168^{+28}_{-24} from Bertout et al. (1999) (calculated by HIPPARCOS measurements of 4 members of Cha I and resulting in an average distance of 168^{+14}_{-12} to the cloud), we find luminosities $\log(L/L_\odot)$ of -1.21 ± 0.14 and -1.25 ± 0.14, and radii of $0.92^{+0.19}_{-0.14}$ and $0.88^{+0.18}_{-0.13}$ $R_\odot$ for Cha Hα 2 A (SW) and B (NE), respectively. This makes both components more massive than the more massive component of the eclipsing binary brown dwarf found by Stassun et al. (2006) in Orion of $M = 0.054 \pm 0.005$ $M_\odot$ (assuming similar age, which is justified).

It is, a priori, not known to which of both components the photometric rotation period refers. However, since both stars are very young and have been formed in similar environmental conditions, we may assume that they rotate at the same speed. In this case, we can conclude from the photometric period of 3.21 ± 0.17 days (Joergens et al. 2003) and the $v \sin i$ of 12.8 ± 1.2 km s^{-1} (Joergens & Guenther 2001) that Cha Hα 2 A and B have inclinations of 36.1 to 143.9 deg and 40.4 to 139.6 deg, respectively, consistent with ~65 to 75 deg by Natta et al. (2004). Assuming an alignment of the orbital axis and the rotational axis of both components, this is also consistent with our finding of astrometric orbital motion in the form of a change in separation rather than in a change of the PA, i.e., with an orbital plane being more edge-on than pole-on.

Given the luminosities, temperatures, radii, and gravities, the masses of both components are $0.308^{+1.430}_{-0.231}$ $M_\odot$ and $0.281^{+1,302}_{-0.210}$ $M_\odot$ for A and B, thus leaving Cha Hα 2 AB above the stellar – brown dwarf boundary. However, component B could still be a brown dwarf, according to this error estimation. Although we arrive at masses that could possibly be higher than the sun's (given our large error bars), this can be ruled out due to the fact that such very young objects could be of approximately same size as the sun, but would not have a similar surface gravity at the same time. Using theoretical models by Baraffe et al. (1998), we find a best fit for masses of 0.124 $M_\odot$ and 0.110 $M_\odot$ for Cha Hα 2 A and B for an age of 2 Myr, a temperature of ~3025 K, a log g of ~3.6, and the luminosity values as derived above of $\log(L/L_\odot)$ of −1.21 and −1.25, but we would like to mention that the determination of ages and masses from evolutionary models is uncertain until at least 10 Myr (Chabrier et al. 2005). These mass values are in good agreement with the mass for the unresolved Cha Hα 2 of 0.14 $M_\odot$ from Mohanty et al. (2005). While there are currently almost one hundred systems known of even lower total mass (Siegler 2007), a review of the field and the existence of very low mass binaries at different ages can be found in Burgasser et al. (2007).

After submission of our manuscript Ahmic et al. (2007) reported the possible binarity of Cha Hα 2 found in their data from 2005, included as 1st epoch in our common proper motion analysis. We note that separation, position angle, and *Ks*-band magnitudes measured coincide well within the 1σ error bars of each other. Ahmic et al. (2007) could not show common proper motion because they had only one epoch available.

The projected separation between A and B corresponds to ~27 AU at ~168 pc, so that further investigation of the interaction between the two components in Cha Hα 2 and its disk (with silicate feature) would be very important.

Acknowledgements. T.O.B.S. acknowledges support from Evangelisches Studienwerk e.V. Villigst.
Moreover he would like to thank F. Comerón for providing FORS1 images as well as an electronic optical spectrum of Cha Hα 2 from his publication Comerón et al. (2000), P. Hauschildt for the electronic GAIA models, J. Kainulainen for the electronic extinction map of the Cha I cloud for accurate reading of the extinction values, an anonymous referee for helpful comments and Amy Mednick for language editing.
N.V. acknowledges support by FONDECYT grant 1061199.
A.B. and R.N. would like to thank DFG for financial support in projects NE 515/13-1 and 13-2.
This publication makes use of data products from the Two Micron All Sky Survey, which is a joint project of the University of Massachusetts and the Infrared Processing and Analysis Center/California Institute of Technology, funded by the National Aeronautics and Space Administration and the National Science Foundation.
We use imaging data from the SuperCOSMOS Sky Survey, prepared and hosted by Wide Field Astronomy Unit, Institute for Astronomy, University of Edinburgh, which is funded by the UK Particle Physics and Astronomy Research Council.
This research has made use of the VizieR catalogue access tool and the Simbad database, both operated at the Observatoire Strasbourg.

References

Ahmic, M., Jayawardhana, R., Brandeker, A., et al. 2007, [arXiv:0708.3851]
Apai, D., Pascucci, I., Henning, T., et al. 2002, ApJ, 573, L115
Apai, D., Pascucci, I., Bouwman, J., et al. 2005, Science, 310, 834

Baraffe, I., Chabrier, G., Allard, F., & Hauschildt, P. H. 1998, A&A, 337, 403
Bertout, C., Robichon, N., & Arenou, F. 1999, A&A, 352, 574
Brott, I., & Hauschildt, P. H. 2005, in ESA SP, 576, ed. C. Turon, K. S. O'Flaherty, & M. A. C. Perryman, 565
Burgasser, A. J., Reid, I. N., Siegler, N., et al. 2007, in Protostars and Planets V, ed. B. Reipurth, D. Jewitt, & K. Keil, 427
Chabrier, G., Baraffe, I., Allard, F., & Hauschildt, P. H. 2005, ArXiv Astrophysics e-prints
Comerón, F., Neuhäuser, R., & Kaas, A. A. 2000, A&A, 359, 269
Ducourant, C., Teixeira, R., Périé, J. P., et al. 2005, A&A, 438, 769
Gaedke, A. 2005, Diploma thesis, FSU Jena
Golimowski, D. A., Leggett, S. K., Marley, M. S., et al. 2004, AJ, 127, 3516
Joergens, V., & Guenther, E. 2001, A&A, 379, L9
Joergens, V., Fernández, M., Carpenter, J. M., & Neuhäuser, R. 2003, ApJ, 594, 971
Kainulainen, J., Lehtinen, K., & Harju, J. 2006, A&A, 447, 597
Lenzen, R., Hartung, M., Brandner, W., et al. 2003, in Instrument Design and Performance for Optical/Infrared Ground-based Telescopes, ed. M. Iye, & A. F. M. Moorwood, Proc. SPIE, 4841, 944
Luhman, K. L. 1999, ApJ, 525, 466
Luhman, K. L. 2004, ApJ, 616, 1033
Mohanty, S., Jayawardhana, R., & Basri, G. 2005, ApJ, 626, 498
Monet, D. G., Levine, S. E., Canzian, B., et al. 2003, AJ, 125, 984
Natta, A., & Testi, L. 2001, A&A, 376, L22
Natta, A., Testi, L., Muzerolle, J., et al. 2004, A&A, 424, 603
Neuhäuser, R., & Comerón, F. 1998, Science, 282, 83
Neuhäuser, R., & Comerón, F. 1999, A&A, 350, 612
Neuhäuser, R., Brandner, W., Alves, J., Joergens, V., & Comerón, F. 2002, A&A, 384, 999
Rieke, G. H., & Lebofsky, M. J. 1985, ApJ, 288, 618
Rousset, G., Lacombe, F., Puget, P., et al. 2003, in Adaptive Optical System Technologies II, ed. P. L. Wizinowich, & D. Bonaccini, Proc. SPIE, 4839, 140
Siegler, N. 2007, in Proc. of the Conf. In the Spirit of Bernard Lyot: The Direct Detection of Planets and Circumstellar Disks in the 21st Century, June 04–08 2007 (Berkeley, CA, USA: University of California), ed. P. Kalas., 45
Stassun, K. G., Mathieu, R. D., & Valenti, J. A. 2006, Nature, 440, 311
Stelzer, B., Micela, G., & Neuhäuser, R. 2004, A&A, 423, 1029

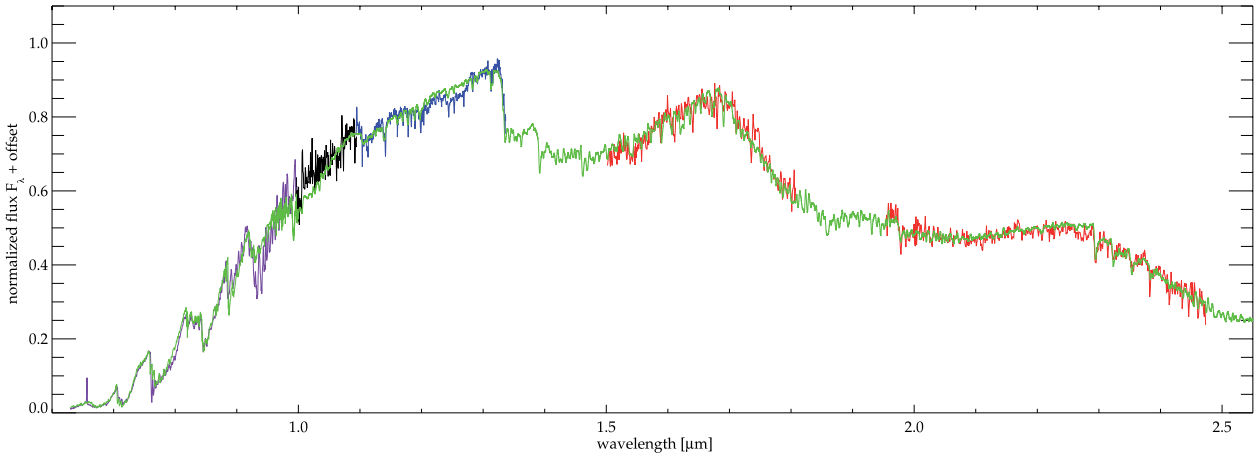

Fig. 6. Spectrum of both components from the optical part to the near-infrared combined from data from Comerón et al. (2000) (purple), and data from the ESO Paranal and La Silla instruments ISAAC (blue) and SofI (black: blue arm spectra, red: red arm spectra) retrieved from the ESO Science Archive Facility. The best fit to the spectrum, a GAIA model computed with the PHOENIX code by Brott & Hauschildt (2005) for a temperature of 3000 K, log g of 4.0 and a visual extinction of 4.3 mag is superimposed in green. Note that the missing flux depression in J-band (between 1.2 and 1.3 micron) as well as in the peak of the H-band (around 1.65 micron) is due to missing FeH opacities in the spectral models. Note the strong Hα emission in Cha Hα 2 at 0.6568 μm.